

Received 30 September 2024, accepted 24 October 2024, date of publication 30 October 2024, date of current version 8 November 2024.

Digital Object Identifier 10.1109/ACCESS.2024.3488072



## RESEARCH ARTICLE

# Promoting by Looking Into Friend Circles: An Inadequately-Labeled and Socially-Aware Financial Technique for Products Recommendation

NAN SU<sup>ID</sup>

School of Finance and Trade, Zhengzhou Shengda University, Zhengzhou, Henan 451191, China

e-mail: 100259@shengda.edu.cn

**ABSTRACT** We have developed a classification method that segments a large group of Amazon or TikTok users into distinct categories, or “genres,” based on their shared purchasing behaviors, such as preferences for consumer electronics or household items. Our approach uses a geometry-based feature selection strategy to accurately capture each user’s buying patterns, which are characterized by a range of features, including those learned under weak supervision. These features are then refined through two feature selection processes tailored to different application needs. We also use a probabilistic model to represent each user’s buying preferences as a distribution within a hidden feature space. To map the purchasing connections between users, we construct a graph and apply a specialized algorithm to identify tightly connected subgroups. These subgroups reflect shared purchasing habits, allowing us to categorize users into specific genres. Finally, a ranking model is used to recommend products to users based on these genres. We validated the effectiveness of our recommendation system using a dataset of over one million Amazon users, showing that it accurately identifies and classifies distinct purchasing genres.

**INDEX TERMS** Genre, online products, weak supervision, graph mining, social connection, purchasing preference.

## I. INTRODUCTION

As personal mobile devices and internet access continue to grow, the number of global digital consumers is expected to reach 2.14 billion, accounting for a quarter of the world’s population. This surge in online shoppers, combined with the vast selection of products available, highlights the competitive advantage of online shopping platforms. Their success increasingly depends on effectively matching the right products to the right customers, making product recommendation systems more important than ever. These systems typically fall into two main types: 1) Collaborative Filtering: This method recommends products based on a customer’s past interactions (such as ratings, views, or purchases) and the behaviors of similar users. For example, if customers

The associate editor coordinating the review of this manuscript and approving it for publication was Wei Wei<sup>ID</sup>.

who bought a football jersey also purchased soccer balls, the system might suggest a soccer ball to a similar customer. 2) Item-based Filtering: This approach suggests products by comparing the features of items a customer has shown interest in. For instance, a soccer ball might be recommended because it shares certain features with a football jersey the customer previously bought.

In the past decade, platforms like Facebook, Twitter, and Amazon have turned social media into a valuable tool for understanding customer preferences and purchasing behaviors. By capturing customer sentiments and intentions, these platforms provide deep insights into buying patterns. Recently, personality computing has emerged as a new way to enhance user modeling and recommendation systems by incorporating individual personality traits into the process.

TikTok, for example, has become a vibrant platform for sharing and recommending products, with users forming

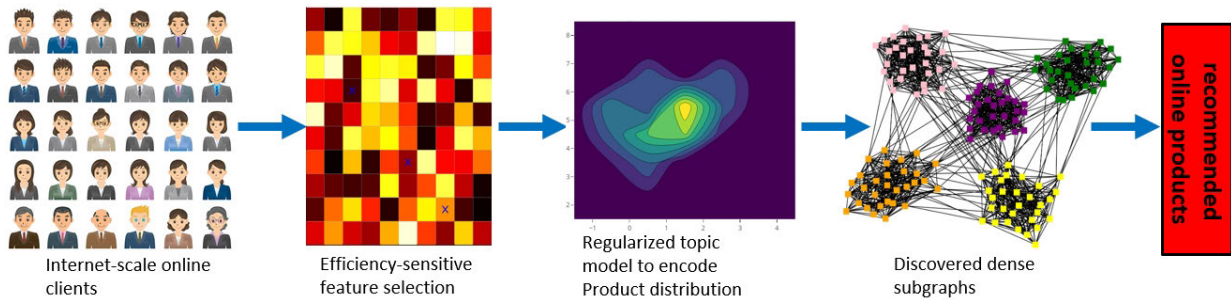


**FIGURE 1.** The overview of the proposed weakly-supervised online product recommendation architecture.

groups around specific shopping interests. These groups, which can include thousands of members, play a key role in spreading product recommendations to a wide audience. Users can freely join or leave groups or even create new ones. However, the current process of forming these groups is manual and basic, pointing to the need for an automated system that can intelligently categorize users based on their shopping preferences. Developing such a system presents challenges, as it requires innovative approaches to effectively analyze and leverage user data and preferences.

- Computational models used to assess customers' purchasing preferences need to be built with features that are specifically relevant to the demographics being analyzed. For example, younger customers may prefer popular electronic products like the Apple Vision Pro or iPhone 15 and often share images of these on their TikTok profiles. In contrast, middle-aged consumers tend to favor healthy foods and household items. This highlights the need for a smart online product recommendation system that can adapt to different client segments by integrating diverse text, semantic, and visual features.
- The number of photos customers upload can vary widely; some might share over 8,000 images of purchased products, while others may have interacted with fewer than five products online. These discrepancies in data contributions create challenges when training a reliable model for product recommendations, as they can lead to issues like overfitting and imbalanced data.

To address these challenges, we propose a weakly-labeled regularized topic model that accurately captures clients' purchasing behaviors. We begin by extracting a comprehensive set of textual, semantic, and visual features that represent each client's preferences. These features are then integrated into a probabilistic topic model, which represents each client's interests as a distribution across various categories. To prevent overfitting, especially for clients with limited data, we include a regularization term in the model. Additionally, we use KL-divergence to measure the similarity between clients' purchasing preferences, constructing an affinity graph that captures these relationships. Clients with similar interests, as indicated by their position in the graph, are grouped into distinct purchasing categories using a dense

graph mining technique. Finally, a ranking mechanism based on similarity metrics is applied to recommend the most relevant products to each client. The core components of our recommendation system are illustrated in Fig. 1.

Our research offers four key contributions: 1) We developed a regularized topic model that effectively combines diverse features to capture user purchasing preferences. 2) We created a graph-based ranking system to efficiently recommend products. 3) We introduced a weakly-supervised learning framework that links client tags to their product representations. 4) We performed extensive experiments to validate the effectiveness of our recommendation system.

This document is organized as follows: Section II reviews relevant literature. Section III outlines our methodology, including the calculation of purchasing-related features, the creation of a large-scale graph to represent client purchasing relationships, and the graph-based categorization and ranking system for product recommendations. Section IV presents experimental results that demonstrate the system's effectiveness. Section V concludes the paper by summarizing our findings and suggesting future research directions.

## II. REVIEWING THE RELATED WORK

### A. CUSTOMIZED PRODUCT RECOMMENDATIONS

Extensive research has shown that understanding user characteristics can significantly improve the effectiveness of product recommendations. For example, one study [64] developed a framework that recommends video content by analyzing users' Big Five personality traits through text mining, successfully matching games with players' dominant traits in a study of 2400 gamers on Steam. Another study [66] introduced a character-based re-ranking technique to tailor recommendation lists to diverse user preferences. Similarly, [67] created a platform for recommending potential friends by combining personality profiling with advanced filtering techniques, focusing on compatibility and interests. In another study, [68] explored the connection between personality modeling and acoustic features, analyzing data from 1415 Last.fm users, which included personality tests and music preferences. A subsequent validation study [69] examined the Tune-A-Find app, where users selected music based on factors such as activity, mood, and expertise, demonstrating the value of personality traits in recommendations.

Additionally, [70] implemented a Collaborative Filtering (CF) framework using personality modeling to group users, improving prediction accuracy in sparse data scenarios. Dai et al. [71] emphasized the role of social attributes, viewed as digital personas, in enhancing engagement and accuracy in recommendation systems. Khelloufi et al. [72] also explored how leveraging social characteristics can improve service recommendations in IoT environments, highlighting the expanding role of character modeling in various recommendation systems.

Our approach differs from previous methods by focusing on segmenting users based on their purchasing behaviors rather than primarily on personality traits or social attributes. While earlier studies like [64], [66], and [67] relied on personality traits for content recommendations, and others like [68] and [69] explored links between personality and behaviors (such as music preferences), our method takes a different path. We use a geometry-based feature selection strategy to capture users' buying tendencies, with features learned through weak supervision. By employing a probabilistic model, we represent purchasing preferences within a hidden feature space and construct a graph that depicts the relationships among clients, grouping them into genres based on shared behaviors. Tested on over a million Amazon users, our method effectively identifies distinct purchasing genres and recommends products based on buying patterns rather than personality or social traits.

### B. EXPLORING USER INTERESTS AND PREFERENCES

Significant research has focused on identifying user interests by leveraging socially-aware features. One study [13] provided an in-depth review of discovering client interests on Facebook, including methods for data collection, constructing, refining, and evaluating user interest profiles. Another study [14] introduced a visual model that predicts purchasing tendencies by considering user contributions (both explicit and implicit), connections between users, and topic similarities. Similarly, [15] explored detecting hidden purchasing tendencies through frequent pattern mining, focusing on topic alignment without modeling deeper connections between topics. Meanwhile, [16] applied a regularization method using a bipartite graph based on social networks from retweet patterns. Dhelim et al. [17] examined how user interests could personalize services in an intelligent home environment. Reference [18] introduced Twixonomy, which organizes Amazon clients by using hierarchical categories based on hidden purchasing behaviors, linking users' interests to Wikipedia pages. Reference [19] used socially-aware content analysis to extract users' topical interests, while [20] developed an algorithm to align social media content with news categories, using Wikipedia to enrich user profiles. Lastly, [21] presented iExpansion, a filtering algorithm that improves user interest detection through personalized ranking, using a three-tier architecture to enhance recommendation accuracy and reduce computational costs.

Previous methods focus on using socially-aware features and user interactions to extract interests and improve recommendations, such as [13], [14], and [15], which rely on user contributions, topic similarities, and pattern mining. Others, like [18] and [19], use social media content to categorize users based on implicit interests. In contrast, our approach segments users into "genres" based on their purchasing behaviors, independent of social connections. We use a geometry-based feature selection strategy, weak supervision, and a probabilistic model to represent user preferences in a hidden feature space. We also construct a graph of purchasing connections and group users into genres using a subgraph extraction algorithm. Our method focuses specifically on purchasing behavior and has been tested on over one million Amazon users to provide effective product recommendations.

### C. COMMUNITY IDENTIFICATION AND SOCIALLY-AWARE RECOMMENDATION

Recent advancements in community identification have utilized Gaussian probabilistic models like LDA [30] and its variants [41], [42] to detect socially-aware groups. These models treat social networks as generative processes, where users are categorized into communities based on shared link patterns and distributions. Zhou et al. [43] and Yin et al. [44] expanded these models to include semantic content, treating communities as clusters of topics that emerge from both social interactions and content analysis. This combined approach, which uses both textual content and structural patterns within networks, has been effective in defining clearer community boundaries and shows the flexibility of probabilistic models in uncovering complex social structures shaped by both semantic content and network data.

Our approach differs from previous work by focusing on segmenting users based on purchasing preferences, using geometry-based feature selection and probabilistic modeling. We construct a graph of purchasing connections and group users into "genres" based on their buying behavior, validated on a large dataset to enhance product recommendations, with a focus on purchasing data rather than social interactions.

Pecune et al. [34] introduced a conversational recommender system that uses socially-aware interactions for personalized recipe suggestions, increasing user engagement by considering social context. Du et al. [35] addressed the cold-start problem in recommendation systems through socially-aware contrastive learning, which uses social relationships to improve recommendations when data is limited. Konomi et al. [36] explored living trust networks for socially-aware recommendations, emphasizing the role of user trust and social ties in generating reliable suggestions. Another work by Pecune et al. [37] focused on persuasive conversational systems in the food domain, using nudging techniques and social awareness to influence users' decisions. Yu et al. [38] proposed a socially-aware self-supervised learning approach to improve recommendations

by leveraging implicit social signals. Lee and Hong [39] studied socially-aware joint recommendation and caching policy design in wireless device-to-device networks, optimizing performance by combining social data with network characteristics. Lastly, Dhelim et al. [40] provided a comprehensive survey on personality-aware recommendation systems, highlighting the potential of using personality traits to improve recommendation accuracy. Together, these studies demonstrate the growing importance of socially-aware and context-rich models in improving recommendation systems and user satisfaction across various applications.

### III. TECHNIQUE OVERVIEW

#### A. INTEGRATING VISUAL AND PURCHASING-RELATED FEATURES WITH WEAK SUPERVISION

To represent each product comprehensively, we use a nine-dimensional color moments descriptor [47] and a 64-dimensional Histogram of Oriented Gradients (HOG) [46] to capture key visual features from product images. These vectors are combined into a single image descriptor using max pooling [26], resulting in a 265-dimensional feature vector. Nine dimensions from color moments and 256 from the combined HOG and semantic vectors. Additionally, we include a 128-dimensional deep CNN feature for further visual representation, following the approach in [23]. To capture purchasing-related features, we apply a weakly-supervised learning method based on a “bag of samples” approach. In this method, multiple online products are grouped into “bags” with only a weak indication of which samples are relevant. Each bag contains several products, with a label assigned to the entire bag rather than to individual products. The label indicates whether the bag contains at least one relevant product, without specifying which one. In our approach, each bag is assigned a four-dimensional weak label vector, and we use the objective function from [29] to transfer these weak labels to each product using a manifold-based feature projection. As a result, each product is represented by a 64-dimensional semantic feature. Combining all features, each product image is ultimately described by a 457-dimensional feature vector, which integrates visual, semantic, and weakly-labeled purchasing-related features.

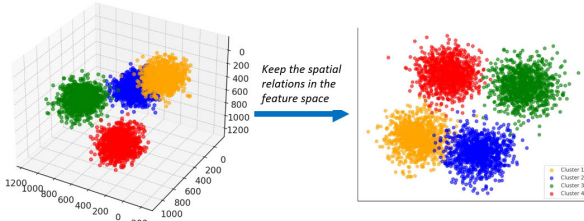


**FIGURE 2.** Visualization of Preserving Spatial Relations Among Samples in Feature Selection Process.

#### B. REGULARIZED FEATURE SELECTION FOR IMAGE CATEGORIZATION

In this framework,  $\mathbf{F} = [f_1, \dots, f_N] \in \mathbb{R}^{N \times T}$  denotes the matrix containing composite features for all training

products on social media, where  $\mathbf{F}_L = [f_1, \dots, f_L]$  represents the features of the first  $L$  labeled images, and  $\mathbf{F}_U = [f_{L+1}, \dots, f_N]$  covers those of the unlabeled images. The labels for these images are captured in  $\mathbf{M} = [m_1, \dots, m_L]$ .

Introducing  $\mathbf{P} \in \mathbb{R}^{T \times C}$ , with  $C$  indicating the number of image categories, this matrix helps prioritize features during classification. In our method,  $T$  denotes the number of selected features and  $N$  means the total labeled samples during feature selection. The objective function for our feature selection is structured as follows:

$$\min_{\mathbf{P}} \epsilon(\mathbf{P}) + \varphi \cdot \eta(\mathbf{P}), \quad (1)$$

where  $\epsilon(\mathbf{P})$  acts as the loss function, measuring prediction errors, and  $\varphi \cdot \eta(\mathbf{P})$  imposes a regularization penalty to prevent overfitting.

We utilize an adjacency matrix  $\mathbf{W}$ , where each  $\mathbf{W}_{ij}$  measures the similarity between sample points  $i$  and  $j$ . If closely related,  $\mathbf{W}_{ij}$  is set to 1; otherwise, it's 0. The diagonal matrix  $\mathbf{D}$ , with each  $\mathbf{D}_{ii}$  summing the  $i$ -th row of  $\mathbf{W}$ , forms the graph Laplacian  $\mathbf{L} = \mathbf{D} - \mathbf{W}$ , helping preserve geometric relationships among data points, crucial for maintaining feature space integrity as shown in Fig. 2.

Our method employs both labeled and unlabeled data, applying transductive learning principles [24] to spread label information across the dataset. Define  $\mathbf{J} = [j_1, j_2, \dots, j_N]^T \in \mathbb{R}^{N \times C}$ , where each  $j_i$  is a predicted label vector for the  $i$ -th sample. The goal is to refine  $\mathbf{J}$  to closely match true labels  $\mathbf{M}$  for labeled samples and respect structural constraints denoted by  $\mathbf{W}$ , aiming to optimize:

$$\arg \min_{\mathbf{J}} \text{tr}(\mathbf{J}^T \mathbf{K} \mathbf{J}) + \text{tr}((\mathbf{J} - \mathbf{L})^T \mathbf{V} (\mathbf{J} - \mathbf{L})), \quad (2)$$

Here,  $\mathbf{J}$  accentuates differences between labeled and unlabeled samples; it's set very high for labeled samples to emphasize their influence and at 1 for unlabeled ones. This strategy uses known classifications to guide the learning process, focusing on minimizing the discrepancies between calculated labels and the ground truth, thus enhancing label prediction accuracy for unlabeled images. By accommodating both data types within an affinity graph framework, this method leverages the dataset's full characteristics, enabling refined predictions across all images.

$$\begin{aligned} & \arg \min_{\mathbf{J}, \mathbf{G}} \text{tr}(\mathbf{J}^T \mathbf{K} \mathbf{J}) + \text{tr}((\mathbf{J} - \mathbf{L})^T \mathbf{V} (\mathbf{J} - \mathbf{L})) \\ & + \beta \|\mathbf{G}^T \mathbf{P}\|_F^2 + \varphi \cdot \eta(\mathbf{P}), \end{aligned} \quad (3)$$

In these equations, the incorporation of the  $l_{2,1/2}$ -norm serves as a non-convex Hessian regularizer, adding a layer of complexity to the optimization challenge. A non-convex Hessian regularizer improves optimization by using the curvature information of a function, captured through the Hessian matrix, to guide the solution process. In non-convex problems, where multiple local minima and saddle points exist, the regularizer helps control the function's curvature, making the optimization landscape smoother and more stable. This reduces the likelihood of the optimizer getting stuck

in poor local minima. Hessian-based regularization is often combined with methods like Newton-type algorithms or their approximations, which leverage second-order information to improve convergence. Although it doesn't ensure finding the global minimum, Hessian regularization enhances the optimizer's ability to find better local minima in challenging, high-dimensional problems.

To effectively manage this complexity, we adopt an iterative approach specifically designed to tackle non-convex problems, as detailed in [25] and [65]. This methodology meticulously refines the feature selection process, ensuring that the implementation remains both practical and efficient within the framework of a Hessian-regularized setting. This strategic integration of advanced regularization techniques substantially enhances the robustness of the optimization, leading to more reliable feature selection and ultimately more accurate modeling outcomes.

### C. TIME-EFFICIENT FEATURE SELECTION FOR MOBILE PLATFORMS

In environments that demand rapid responses, such as mobile applications, our recommendation system uses a time-aware feature selector. This selector evaluates each feature based on three main criteria: the computation time required, its effectiveness in distinguishing scenarios, and the relationships among features. Computation time is split into the duration for feature extraction and classification. We record both times to evaluate each feature's overall processing time.

The discriminative power of a feature is assessed using the feature margin, which measures how well the feature distinguishes between classes. The margin is based on the difference between a feature's distance to the nearest miss (a sample from a different class) and the nearest hit (a sample from the same class). A higher score indicates stronger discriminative ability.

Additionally, feature correlation is analyzed to identify overlaps or redundancies. When two features have high correlation but both show strong discriminative capabilities, one feature may be removed to reduce dimensionality and improve system efficiency. This correlation is quantified using information gain, based on entropy. The aim is to balance feature effectiveness with computational efficiency by discarding redundant features.

To optimize feature selection, we introduce the discrimination-time ratio (DTR), which balances discriminative power against time cost. Features with a higher DTR score are more efficient. Similarly, the time-correlation ratio (TCR) assesses the trade-off between processing time and feature redundancy, ensuring that only the most unique and time-efficient features are retained.

Finally, non-linear transformations are applied to features to reveal deeper relationships, and both DTR and TCR metrics are used to evaluate these transformed features. Our feature selection method, called DTR & TCR-based

Feature Selection, operates in two phases: first, it removes features with low discriminative power using DTR, and then eliminates highly redundant features using TCR, thus enhancing the performance and speed of the recommendation system.

### D. ADVANCED LATENT TOPIC MODELING FOR CLIENT PURCHASING BEHAVIOR

In this section, we introduce a method to model each client by the distribution of their purchased products, employing a sophisticated latent topic model. We enhance traditional approaches by integrating Gaussian Mixture Models (GMMs) and Probabilistic Latent Semantic Analysis (PLSA) [48], which allows for more refined modeling of density distributions. In our model, each latent variable  $z$  corresponds to a Gaussian component responsible for generating the observable data point  $\mathbf{x}$ . This approach captures the principal characteristics of each online product, enabling us to thoroughly characterize the dataset  $\mathbf{X} = \{\mathbf{x}_1, \mathbf{x}_2, \dots, \mathbf{x}_N\}$  and effectively encapsulate the intricate thematic nuances of the images within a probabilistic framework.

$$p(\mathbf{X}|\alpha, \beta, \Gamma) = \prod_{i=1}^N \sum_{w=1}^W p(w|\alpha)p(\mathbf{x}_i|\beta_w, \Gamma_w), \quad (4)$$

In this model,  $p(w|\alpha)$  represents the mixture coefficients, while  $p(\mathbf{x}_i|\beta_w, \Gamma_w)$  specifies the Gaussian probability distribution for the  $w$ -th component.

Probabilistic Latent Semantic Analysis (PLSA) [48] offers a probabilistic method to explore topic distribution across diverse texts. In PLSA, each topic is encapsulated by a latent variable  $z$ , suggesting that each distinct feature  $t$ , viewed as an aesthetic or thematic element, occurs independently of the document  $d$  in which it is found. The overall probability of encountering these variables is expressed in their joint distribution, which is described as follows:

$$p(d_i, t_j) = p(d_i) \sum_{k=1}^K p(k|d_i)p(t_j|k), \quad (5)$$

In the Latent Semantic Analysis (LSA) framework,  $p(k|d_i)$  represents the probability of encountering the genre  $k$  within a specific document  $d$ , and  $p(t_j|k)$  denotes the likelihood of observing the refined feature  $t$  associated with that genre. Traditional LSA, however, is primarily designed for discrete data and often faces challenges when dealing with the continuous nature of purchasing preferences in online product data. To overcome these limitations, we utilize Gaussian Mixture Models (GMMs), which are highly effective for modeling continuous data distributions, to develop a Gaussian Latent Topic Model that extends the conventional LSA framework.

This advanced model conceptualizes the continuous refined features in images as outcomes of various Gaussian distributions. In this configuration, each feature vector  $\mathbf{x}$  within a product image  $d$  corresponds to a specific Gaussian component  $w$ , which is associated with a product tag  $a$ . For our extensive dataset of online products, the composite distributions are defined by the following

model configuration:

$$p(\mathbf{X}|\Sigma) = \prod_{d=1}^M \prod_{i=1}^N \sum_{k=1}^K \sum_{w=1}^W p(z^{(d,i)}|\sigma_d) p(w^{(d,i)}|\phi_a) p(\mathbf{x}^{(d,i)}|\beta_{w,a}, \Gamma_{w,a}), \quad (6)$$

In the Latent Semantic Analysis (LSA) framework,  $p(k|d_i)$  represents the probability of encountering the genre  $k$  within a specific document  $d$ , and  $p(t_j|k)$  denotes the likelihood of observing the refined feature  $t$  associated with that genre. Traditional LSA, however, is primarily designed for discrete data and often faces challenges when dealing with the continuous nature of purchasing preferences in online product data. To overcome these limitations, we utilize Gaussian Mixture Models (GMMs), which are highly effective for modeling continuous data distributions, to develop a Gaussian Latent Topic Model that extends the conventional LSA framework.

This advanced model conceptualizes the continuous refined features in images as outcomes of various Gaussian distributions. In this configuration, each feature vector  $\mathbf{x}$  within a product image  $d$  corresponds to a specific Gaussian component  $w$ , which is associated with a product tag  $a$ . For our extensive dataset of online products, the composite distributions are defined by the following model configuration:

$$\begin{aligned} R(\Omega|\Omega^p, \Omega_H^p) \\ = p(\mathbf{X}|\Sigma) \\ + \sum_{d=1}^M \sum_{i=1}^N \sum_{k=1}^K \sum_{w=1}^W p(a, w|\Omega^p) \log \frac{p(\mathbf{x}^{(d,i)}, a, w|\Sigma)}{p(\mathbf{x}^{(d,i)}, a, w|\Sigma^p)} \\ + \kappa \sum_{d=1}^M \sum_{i=1}^N \sum_{a=1}^K \sum_{w=1}^W p(a, w|\Omega_H^p) \log \frac{p(\mathbf{x}^{(d,i)}, a, w|\Sigma)}{p(\mathbf{x}^{(d,i)}, a, w|\Omega_H^p)} \\ \propto \text{EXP}_{q_r(a, w|\mathbf{X}, \Omega^p, \Omega_H^p)} [\log p(\mathbf{X}, a, w|\Omega)], \end{aligned} \quad (7)$$

where  $\kappa$  denotes a non-negative weighting factor.  $\Omega_H = \{\alpha_H, \pi\}$ ,  $\Sigma_H = \{\alpha_H, \pi, \beta, \Gamma\}$ .  $q_r(a, w|\mathbf{X}, \Omega^p, \Omega_H^p)$  denotes the regularization distribution across the latent variables, specifically,

$$q_r(a, w|\mathbf{X}, \Omega^p, \Omega_H^p) = \frac{p(a, w|\mathbf{X}, \Omega^p) + \kappa p(a, w|\mathbf{X}, \Omega_H^p)}{1 + \kappa}. \quad (8)$$

To solve the minimization of the expression using the Expectation-Maximization (EM) algorithm, we can follow these steps:

1. Expectation (E-step): - Compute the posterior probabilities (responsibilities) of the latent variables given the observed data and current parameter estimates. Specifically, we calculate the responsibilities for each component  $w$  and latent variable  $a$  given the observed data  $\mathbf{x}^{(d,i)}$  and current parameters  $\Omega^p$  and  $\Omega_H^p$ . - The responsibilities  $q_r(a, w|\mathbf{X}, \Omega^p, \Omega_H^p)$  can be computed using the following formula:

$$q_r(a, w|\mathbf{X}, \Omega^p, \Omega_H^p) = \frac{p(a, w|\mathbf{X}, \Omega^p) + \kappa p(a, w|\mathbf{X}, \Omega_H^p)}{1 + \kappa}.$$

- Here,  $p(a, w|\mathbf{X}, \Omega^p)$  and  $p(a, w|\mathbf{X}, \Omega_H^p)$  are the posterior probabilities under the current and regularization parameter sets, respectively.

2. Maximization (M-step): - Update the model parameters  $\Omega$  (which includes  $\alpha$ ,  $\beta$ ,  $\Gamma$  and possibly other parameters) by maximizing the expected log-likelihood computed in the E-step. This involves solving the following optimization problem:

$$\max_{\Omega} \sum_{d=1}^M \sum_{i=1}^N \sum_{k=1}^K \sum_{w=1}^W q_r(a, w|\mathbf{X}, \Omega^p, \Omega_H^p) \log p(\mathbf{x}^{(d,i)}, a, w|\Omega).$$

- This step involves updating the parameters such as mixture weights, means, and covariances of the Gaussian components, which can be derived from the weighted sums and averages of the responsibilities computed in the E-step.

3. Convergence Check: - Evaluate the convergence of the algorithm by checking the change in the log-likelihood or a similar criterion. If the change is below a certain threshold, the algorithm has converged. Otherwise, return to the E-step with updated parameters.

The exact implementation details will depend on the specific form of the distributions  $p(\mathbf{x}^{(d,i)}, a, w|\Omega)$  and how the responsibilities are computed in the context of the model's latent variables and data.

## E. DEVELOPMENT OF PURCHASE-RELEVANT SIMILARITY NETWORKS

### 1) ESTABLISHING METRICS FOR CLIENT CONNECTIONS

To effectively map the purchasing connections among various clients, a robust similarity measure is crucial. Utilizing Gaussian Mixture Models (GMMs) from our advanced topic modeling, we represent each user's purchasing preferences with unique Gaussian distributions. To measure the differences between these distributions, we employ the Kullback-Leibler divergence ( $D_{KL}$ ), denoted as  $\mathcal{N}$  and  $\mathcal{N}'$  for two different clients.

Considering the inherent asymmetry of  $D_{KL}$  and the complications it introduces in algorithms that require symmetric matrices, such as spectral clustering, we opt for the square root of the Jensen-Shannon divergence. This symmetrical and more computationally manageable alternative to  $D_{KL}$  is used to assess aesthetic similarities. This modification enhances its integration into our clustering methodologies, thereby strengthening the robustness and effectiveness of our community detection approach.

$$D_{JS}^{1/2}(\mathcal{F}||\mathcal{F}') = \sqrt{\frac{1}{2} (D_{KL}(\mathcal{F}||\mathcal{F}') + D_{KL}(\mathcal{F}'||\mathcal{F})).} \quad (9)$$

This metric effectively captures the purchasing connections among clients, facilitating the identification of client categories with similar buying behaviors using graph-based clustering. We construct an affinity matrix  $\mathbf{W}$ , where each entry at position  $ij$  reflects the calculated similarity between the aesthetic profiles of users  $i$  and  $j$ . This approach helps to systematically group clients based on their purchasing

preferences.

$$\mathbf{W}_{ij} = \exp\left(-\frac{D_{JS}(\mathcal{F}_i||\mathcal{F}_j)}{2\psi^2}\right), \quad (10)$$

In this configuration,  $\mathcal{F}_i$  and  $\mathcal{F}_j$  represent the purchasing profiles of clients  $i$  and  $j$ , respectively. Utilizing these profiles, we generate an affinity matrix that serves as the foundation for creating a detailed similarity graph, illustrated in Fig. 3. This graph visually encapsulates the relationships between clients based on their purchasing behaviors.

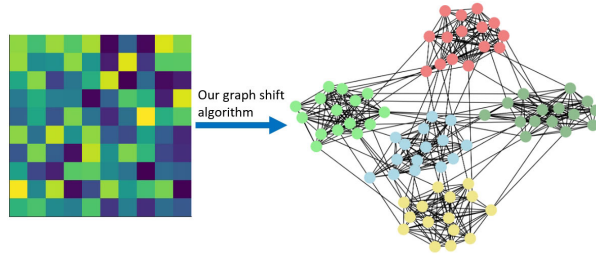


**FIGURE 3.** The left sub figure shows constructing the purchasing affinity graph wherein each element represents the relationships between clients. The Right sub figure shows detecting online product genres by leveraging dense graph mining.

## 2) ENHANCED CLUSTERING OF ONLINE CLIENTS USING GRAPH SHIFTS

Within this approach, we identify dense clusters (i.e., genres) of online clients who share similar purchasing preferences using a graph-based strategy. Key prerequisites include: First, compatibility with our graph-based similarity metric, which relies on color, texture, and semantic connections between users. This metric is particularly suited to graph-based clustering, which naturally handles such pairwise connections. Second, the capability to accommodate outliers with unique tastes that diverge from mainstream purchasing groups.

To effectively discover purchasing genres, we employ the “graph shift” technique, known for its effectiveness in pinpointing densely connected clusters within graph structures. This technique deviates from traditional clustering methods that typically require every client to be categorized. Instead, graph shifting explores the graph structure directly, allowing for an indefinite number of clusters and permitting outliers to remain unclassified. In our defined similarity graph  $\mathbf{G} = (\mathbf{U}, \mathbf{W})$ , where  $\mathbf{U}$  consists of vertices representing online clients and  $\mathbf{W}$  is a symmetric matrix depicting their connections, we analyze the graph’s density function  $g(y) = y^T \mathbf{A}y$  within the simplex  $\Delta^M = y \in \mathbb{R}^M : y \geq 0$  and  $|y|_1 = 1$ . This method not only classifies but also illuminates the depth of connectivity among users within clusters, revealing closely knit communities based on shared aesthetic preferences. This approach skillfully addresses the quadratic optimization challenge to uncover deep connections within the graph, providing a robust framework for community detection.

$$\max_a f(a) = a^T \mathbf{E}a, \quad s.t. \quad a \in \Delta^K, \quad (11)$$

Considering the challenges in deriving an analytical solution for (11), we employ the replicator dynamics technique to identify local maxima. Beginning with an initial state  $a(0)$ , we systematically approach the local optimum  $a^*$  through the discrete-time application of first-order replicator dynamics, iteratively refining our estimates:

$$a_i(k+1) = a_i(k) \frac{(\mathbf{E}a(t))_i}{a(k)^T \mathbf{E}a(k)}. \quad (12)$$

Utilizing the identified purchasing genres, we recommend products to each client  $c_i$  within the  $i$ -th genre using the subsequent ranking function:

$$\text{rank}(c_i) = \operatorname{argmin}_{g \in G} |f(g) - \mathcal{F}(c_i)|, \quad (13)$$

In this context,  $f(g)$  represents the refined feature for online product  $g$ , and  $\mathcal{F}$  signifies the model parameters derived from products associated with client  $c_i$ . Using the described ranking function, the highest-ranked products are recommended to each client.

## IV. DATA COLLECTION AND GENRE ANALYSIS

### A. COMPILED OF A DIVERSE PURCHASING DATASET

To evaluate the effectiveness of our approach in identifying purchasing-relevant genres, we assembled a comprehensive dataset from Amazon, focusing on 20 significant purchasing genres. Each genre encompasses over 300,000 shared product photographs and about 10,000 active clients. Specifically, we extracted between 50,000 and 70,000 products from approximately 5,000 clients per genre. The variation in the number of photos contributed by individual clients, illustrated in Fig. 4, highlights the necessity for incorporating regularization in our model to effectively manage this variance. The detailed statistics of this dataset are presented in Table 1. In our experimental setup, we divided the dataset, consisting of over 300,000 product photographs and 10,000 clients across 20 genres, into 80% for training and 20% for testing. This split was chosen based on standard machine learning practices, which aim to provide a large enough portion of data for the model to learn effectively while reserving a significant portion for unbiased evaluation. We performed the split at the client level, ensuring that 80% of clients from each genre were included in the training set, with the remaining 20% used for testing. This method prevents the model from seeing any test data during training, ensuring a fair evaluation of performance. Additionally, we maintained genre balance between the sets and used 5-fold cross-validation on the training data to further validate our model and reduce the risk of overfitting. The 80/20 split offers a strong balance between learning and evaluation, providing sufficient data for training while leaving enough unseen data for a meaningful test.

Further, we examined the intersections among these genres, as depicted in Fig. 5. Our analysis indicates that approximately 20% of the genres function predominantly independently, another 60% exhibit moderate overlaps with one or more genres, and the remaining are highly interconnected. Such overlaps are typical and reflect the multi-interest

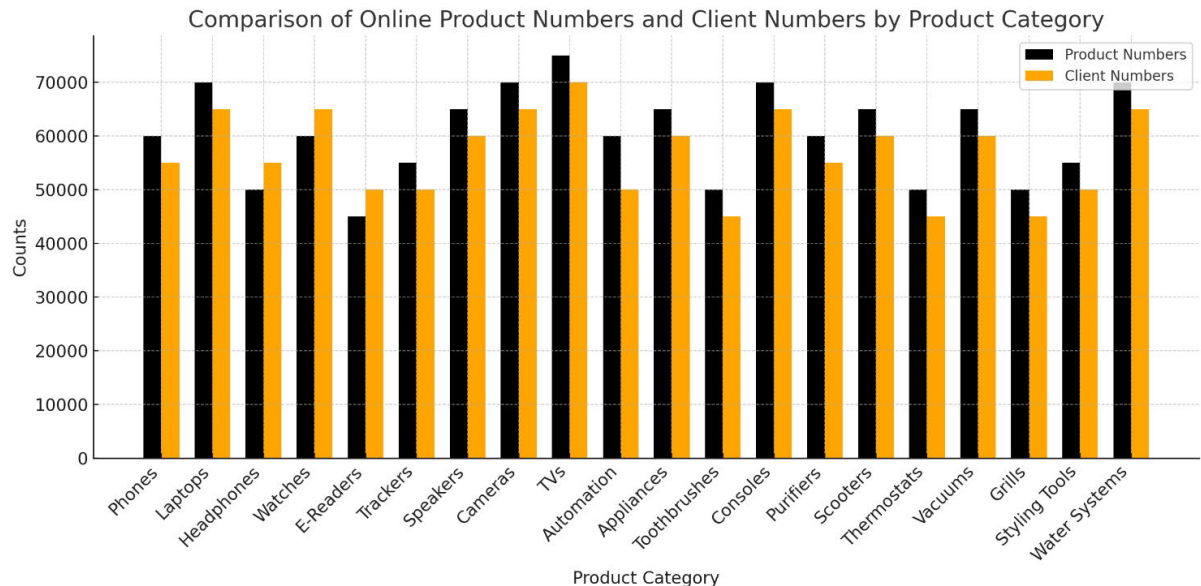


**FIGURE 4.** Distribution of User Numbers Across 20 Purchasing Genres (Horizontal Axis: Groups, Vertical Axis: Client Numbers).

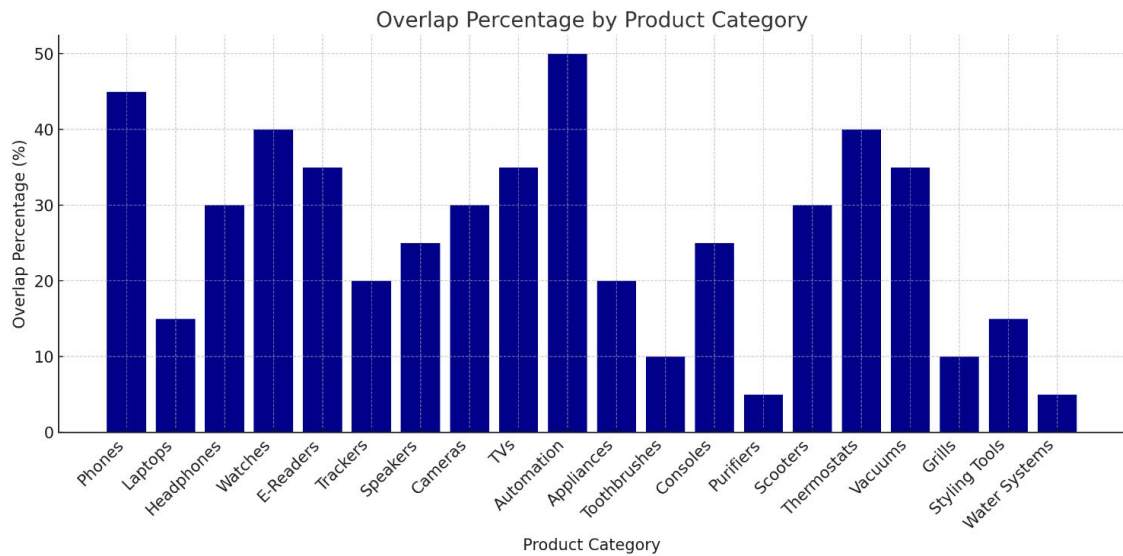


**FIGURE 5.** The Overlapping Percentage of Product Images from the Above 20 Genres.

nature of active clients who participate in multiple groups simultaneously.

### B. A COMPARATIVE STUDY

Our evaluation measures the effectiveness of our purchasing genre identification model  $\mathcal{C} = \{C_1, C_2, \dots, C_Z\}$  against predefined genres  $\bar{\mathcal{C}} = \{\bar{C}_1, \bar{C}_2, \dots, \bar{C}_{\bar{Z}}\}$  using the Balanced Error Rate (BER) [49] to gauge the alignment between the identified and established groups.

To validate our approach, we compare our model against seven renowned clustering algorithms, each emphasizing different analytical dimensions: 1) K-means Clustering; 2) Hierarchical Clustering [45]; 3) Link Clustering [51]; 4) Clique Percolation [50]; 5) Low-Rank Embedding [52]; 6) Multi-Assignment Clustering [53], with each configured to

identify 20 clusters using identical features to those employed in our model.

Key findings, presented in Table 2, reveal: 1) Our model outperforms the other clustering methods in 18 of the 20 genres, evidenced by superior BER scores. This highlights the efficiency of our regularized topic model in accurately delineating user purchasing preferences. 2) Our model achieves more precise genre identification in categories with well-defined themes, such as architecture, compared to more abstract categories like outdoor grills, which pose greater challenges in visual analysis. 3) Our approach shows marked effectiveness in genres with clients who have fewer photo uploads, such as those interested in graphic design or electronic products, demonstrating our model's robustness in managing datasets with significant variations in client activity levels.

**TABLE 1.** Max, Min, Avg photo counts and standard deviation per client.

Genre	Maximum	Minimum	Average	Derivation
Smartphones	2130	19	223	44.6
Hair Styling Tools	1765	21	156	33.4
Laptops	2585	12	265	44.8
Wireless Headphones	3521	20	268	23.4
Water Filtration	2905	18	182	35.3
Smart Watches	5640	44	357	66.0
E-Readers	3655	12	250	43.2
Fitness Trackers	2329	11	145	32.0
Portable Speakers	2985	23	165	47.5
Digital Cameras	4840	2	224	53.2
LED Televisions	3430	28	167	31.3
Home Automation Systems	2750	13	243	45.7
Kitchen Appliances	1755	17	123	49.0
Electric Toothbrushes	3885	22	221	44.3
Gaming Consoles	3120	30	246	38.9
Air Purifiers	3330	33	178	34.7
Electric Scooters	3555	15	256	53.6
Smart Thermostats	4230	31	248	34.1
Robot Vacuum Cleaners	3545	5	243	43.4
Outdoor Grills	3435	19	254	42.2

These results affirm the capability of our proposed model to systematically organize clients into distinct purchasing genres or communities, thereby enhancing our understanding of user interactions and preferences within this digital ecosystem.

### C. EVALUATION OF FEATURE SELECTOR PERFORMANCE

This section examines the effectiveness of our geometry-based feature selector (FS1) and time-sensitive feature selector (FS2) through scene classification tasks, employing high-quality features against four traditional shallow classification frameworks:

1. Fixed-Length Walk Kernel (FWK) and Tree Kernel (FTK) [55]: These kernels excel in recognizing structural image patterns, with FTK extending FWK's scope to hierarchical data structures.
2. Multi-Resolution Histogram (MRH) [62]: Utilizing multi-scale texture analysis, MRH offers a detailed approach to texture-based scene classification.
3. Spatial Pyramid Matching with Kernel Techniques (SPM): This framework includes three variations - Locality-constrained Linear Coding plus SPM (LLC-SPM) [56], Sparse Coding plus SPM (SC-SPM) [57], and Object Bank plus SPM (OB-SPM) [58], each enhancing SPM with unique feature coding strategies for improved scene representation.
4. Super Vector Coding (SVC) and Supervised Image Coding (SSC) [59] [60]: These methods advance image categorization through sophisticated vector quantization and supervised learning techniques, respectively.

The efficacy of our categorization framework is rigorously tested on six diverse scenic image datasets, including well-established benchmarks and newer compilations. Notably:

- Scene-15: This dataset comprises 15 diverse categories, originally compiled by Feifei [5], featuring 200 to 400 images per category with an average resolution of  $320 \times 250$  pixels. The images originate primarily from the COREL database, supplemented by individual photographers and Google Images.

- Scene-67: Focused on indoor scenes, this extensive dataset spans 67 categories, sourced meticulously from Picasa, Altavista, specialized photography sharing sites, and the comprehensive LabelMe database, providing an in-depth look at a wide range of indoor environments.

Additionally, our evaluation extends to four more contemporary scenic image collections that contribute unique perspectives on scenic diversity: -ZJU aerial imagery [4] -ILSVRC-2010 [2] -SUN [6] -Places [1]. These datasets facilitate a thorough assessment of our feature selectors in varying contexts and challenges, allowing us to measure their adaptability and effectiveness across different scene classification scenarios.

To ensure a fair comparison, the configurations for each classification framework were rigorously standardized. For FWK and FTK, parameters were optimized across a range from two to ten to maximize performance. The MRH technique was applied with RBF smoothing at twelve grayscale levels to enhance texture analysis. The SPM approach and its variants analyzed training images using SIFT descriptors on a  $16 \times 16$  pixel grid, followed by creating a 400-term codebook via k-means clustering to develop a sophisticated feature set tailored for scene classification challenges.

With the rapid advancement of multi-layer recognition technologies, a comparative study incorporating the latest deep learning-based scene recognition frameworks was conducted. This review included prominent models such as ImageNet CNN (IN-CNN) [23], Region-based CNN (R-CNN) [11], Meta Object CNN (M-CNN) [12], Deep Mining CNN (DM-CNN) [10], and Spatial Pyramid Pooling CNN (SPP-CNN) [63]. Except for M-CNN [12], all models were evaluated directly without parameter adjustments. For M-CNN [12], the evaluation involved selecting 192 to 384 region proposals per image set via Multiscale Combinatorial Grouping (MCG) [73] and employing a 4096-dimensional feature vector from the FC7 layer of a comprehensive CNN [1]. Additionally, 400 superpixels per scene were generated using the SLIC algorithm [3] and further processed either through a preset linear Discriminant Analysis (LDA) method (SP-LDA) or by selecting 120 visually significant patches identified by the GBV algorithm (SP-GBV). Our RDAL technique enhanced this process by identifying semantically and visually significant superpixels, or Gaze Shift Paths (GSPs), from an array of low-level features, leveraging these GSPs to establish a graph-based superpixel framework forming the basis of our scene classification kernel machine. The superiority of using BING-derived rectangular patches over superpixels is underscored in Tables 3 and 4, highlighting the enhanced descriptiveness of our method. Furthermore, our results were compared against recent advancements in scene classification from [9], [74], and [75], demonstrating the comprehensive adaptability and robustness of our approach.

In our comprehensive quantitative analysis, as detailed in Tables 3 and 4, we rigorously evaluated our model's performance against both cutting-edge deep learning-based and traditional visual recognition frameworks. We conducted

**TABLE 2.** Balanced Error Rate (BER) values for the compared techniques.

Genre	K-means	Hierarchical	Link	Clique Per.	Low-rank	Multi-ass.	Our technique
Smartphones	0.6348	0.4163	0.5432	0.5271	0.4485	0.5061	<b>0.3988</b>
Hair Styling Tools	0.6482	0.5106	0.6369	0.5778	0.5368	0.6120	<b>0.4899</b>
Laptops	0.4648	0.4527	0.4771	0.5100	0.4635	0.4880	<b>0.4403</b>
Wireless Headphones	0.6821	0.7039	0.6712	0.6791	0.7378	0.6910	<b>0.6002</b>
Water Filtration	0.4147	0.4683	0.4361	0.4670	0.4926	0.5090	<b>0.3987</b>
Smart Watches	0.8257	0.7792	0.7859	0.7679	0.7370	0.7687	<b>0.7300</b>
E-Readers	0.6647	0.6879	0.6641	0.6840	0.6779	0.6960	<b>0.5905</b>
Fitness Trackers	0.6100	0.6248	0.5892	0.6062	0.5847	0.6085	<b>0.4890</b>
Portable Speakers	0.7156	0.7259	0.6757	0.6898	0.7069	0.7178	<b>0.5732</b>
Digital Cameras	0.6888	0.7059	0.6851	0.6890	0.7078	0.6656	<b>0.5983</b>
LED Televisions	<b>0.3067</b>	0.4379	0.3447	0.3179	0.2993	0.3534	0.3200
Home Automation Systems	0.6645	0.6799	0.6958	0.6838	0.6791	0.6890	<b>0.5765</b>
Kitchen Appliances	0.7657	0.7841	0.8293	0.7684	0.8204	0.7766	<b>0.7500</b>
Electric Toothbrushes	0.7151	0.7373	0.6889	0.7082	0.7158	0.7598	<b>0.6055</b>
Gaming Consoles	<b>0.3871</b>	0.3879	0.3975	0.4162	0.4276	0.4362	0.4000
Air Purifiers	0.7158	0.7270	0.7078	0.6878	0.6876	0.6950	<b>0.5007</b>
Electric Scooters	0.7658	0.7979	0.8078	0.7950	0.7952	0.8154	<b>0.6600</b>
Smart Thermostats	0.4969	0.4685	0.5259	0.5189	0.4696	0.4850	<b>0.4101</b>
Robot Vacuum Cleaners	0.5357	0.5378	0.5076	0.5185	0.4857	0.4402	<b>0.4308</b>
Outdoor Grills	0.6474	0.6258	0.5987	0.6157	0.6075	0.6270	<b>0.5800</b>
Ave.	0.6199	0.6347	0.6154	0.5951	0.5489	0.6258	<b>0.4956</b>

**TABLE 3.** Mean classification performance of the evaluated models across the mentioned datasets.

Data set	FWK	FTK	MRH	PM	LLC-SP	SC-SP	OB-SP	SV	SSC
Scene-15	72.1%	75.7%	67.2%	77.6%	81.3%	82.5%	77.5%	82.1%	87.4%
Scene-67	41.6%	42.2%	34.6%	44.9%	48.9%	47.7%	48.6%	47.7%	51.7%
ZJU Aerial	66.8%	68.7%	62.5%	73.3%	78.8%	78.1%	78.1%	78.7%	83.0%
ILSVRC-2010	32.5%	30.7%	27.4%	32.8%	38.4%	36.7%	37.2%	37.6%	38.4%
SUN397	15.3%	15.6%	14.2%	22.7%	39.3%	39.5%	38.0%	35.9%	40.6%
Places205	22.5%	22.6%	21.0%	27.9%	31.2%	32.3%	31.6%	31.7%	32.2%
LSDA	47.9%	48.2%	50.6%	47.7%	51.1%	54.5%	47.5%	51.3%	52.7%
Data set	IN-CNN	R-CNN	M-CNN	DM-CNN	SPP-CNN	SP-S	SP-GBV	SP-LDA	Mesnil
Scene-15	83.1%	87.8%	87.7%	89.7%	92.3%	90.9%	86.6%	87.1%	86.4%
Scene-67	57.6%	68.1%	72.3%	68.8%	65.3%	76.6%	71.5%	72.5%	72.2%
ZJU Aerial	75.2%	79.1%	78.6%	81.4%	78.6%	81.2%	80.3%	81.1%	81.0%
ILSVRC-2010	35.7%	38.4%	40.4%	41.0%	41.3%	41.8%	40.4%	40.5%	40.5%
SUN397	48.5%	47.6%	51.6%	48.7%	52.1%	52.1%	50.5%	51.4%	50.5%
Places205	41.1%	44.1%	45.2%	46.3%	48.7%	50.3%	48.4%	48.1%	49.8%
LSDA	52.8%	50.5%	51.8%	53.9%	55.7%	53.0%	58.1%	61.3%	62.1%
Data set	Xiao	Cong	Fast R-CNN	Faster R-CNN	Ours(FS1)	Ours(FS2)			
Scene-15	82.8%	86.6%	90.6%	91.6%	93.5%	92.7%			
Scene-67	71.3%	72.1%	71.5%	74.7%	75.7%	72.9%			
ZJU Aerial	81.1%	80.5%	79.0%	81.6%	84.5%	82.8%			
ILSVRC-2010	40.5%	41.1%	41.2%	41.1%	45.1%	42.3%			
SUN397	50.4%	51.6%	52.2%	52.4%	56.7%	53.2%			
Places205	49.3%	48.6%	48.3%	49.3%	53.1%	51.0%			
LSDA	59.7%	61.5%	62.5%	64.7%	73.9%	72.4%			

**TABLE 4.** Analysis of model performances across the specified datasets.

Data set	FWK	FTK	MRH	SP	LLC-SP	SC-SP	OB-SP	SV	SSC
Scene-15	0.014	0.013	0.014	0.017	0.018	0.019	0.013	0.015	0.014
Scene-67	0.016	0.015	0.017	0.016	0.016	0.015	0.015	0.016	0.016
ZJU Aerial	0.016	0.017	0.018	0.017	0.018	0.017	0.016	0.015	0.016
ILSVRC-2010	0.016	0.015	0.015	0.015	0.016	0.015	0.014	0.015	0.016
SUN397	0.014	0.016	0.016	0.015	0.016	0.017	0.018	0.015	0.017
Places205	0.015	0.016	0.017	0.016	0.018	0.016	0.018	0.017	0.019
LSDA	0.017	0.013	0.017	0.015	0.011	0.014	0.015	0.016	0.015
Data set	IN-CNN	R-CNN	M-CNN	DM-CNN	SPP-CNN	SP-S	SP-GBVS	SP-LDA	Mesnil
Scene-15	0.018	0.015	0.016	0.016	0.017	0.015	0.016	0.015	0.017
Scene-67	0.015	0.017	0.015	0.015	0.016	0.015	0.017	0.015	0.014
ZJU Aerial	0.015	0.016	0.017	0.016	0.015	0.016	0.015	0.018	0.016
ILSVRC-2010	0.017	0.015	0.016	0.015	0.017	0.020	0.015	0.017	0.014
SUN397	0.015	0.016	0.017	0.014	0.016	0.014	0.016	0.016	0.017
Places205	0.014	0.016	0.014	0.015	0.015	0.016	0.015	0.014	0.015
MSEI	0.016	0.014	0.016	0.014	0.016	0.017	0.014	0.019	0.016
Data set	Xiao	Cong	Fast R-CNN	Faster R-CNN	Ours (FS1)	Ours (FS2)			
Scene-15	0.014	0.016	0.015	0.016	0.013	0.014			
Scene-67	0.019	0.014	0.015	0.015	0.008	0.009			
ZJU Aerial	0.016	0.015	0.016	0.014	0.011	0.010			
ILSVRC-2010	0.015	0.015	0.016	0.013	0.010	0.011			
SUN397	0.014	0.015	0.016	0.015	0.009	0.013			
Places205	0.015	0.014	0.016	0.010	0.010	0.011			
LSDA	0.016	0.013	0.017	0.016	0.010	0.011			

each experiment 20 times to ensure the reliability of the results, noting standard deviations to assess the consistency of outcomes. The findings clearly demonstrate that our feature selectors outperform competing methods in terms of classification accuracy and stability.

To further evaluate the effectiveness of our approach in identifying purchasing-relevant genres, we assembled a comprehensive dataset from Amazon, focusing on 45 significant purchasing genres. Each genre encompasses over 601,000 shared product photographs and approximately 20,050 active clients. Specifically, we extracted between 100,000 and 140,000 products from approximately 10,000 clients per genre. The variation in the number of photos contributed by individual clients highlights the necessity of incorporating regularization in our model to manage this variance effectively. The detailed statistics of this expanded dataset are presented in Table 5. The comparative study is reported in Table 6, which clearly demonstrated our method's competitiveness.

#### D. EVALUATION AGAINST ESTABLISHED RECOMMENDATION MODELS

To assess the effectiveness of our newly developed product recommendation system, we compared it with a variety of established models that employ different recommendation strategies. These strategies include deeply-learned models, meta-analytic techniques, large graph mining, and session-guided approaches. Specifically, we evaluated our system against the following models:

**GNN-SEA (Graph Network):** This model treats linkage calculation as a subgraph classification problem. It focuses on the h-hop surrounding subgraph (A) for each potential link (e.g., user-item interactions) and constructs a node information matrix (X) that integrates structural annotations, hidden embeddings, and observable node attributes. These are then processed through a GNN to determine the potential existence of a link, effectively learning from both the graph's structural and nodal attributes. GNN-SEAL's source code is available on GitHub.

**Metapath2vec (Metapath and Network Embedding):** Utilizing metadata-guided random walks, this method generates diverse adjacent nodes for each node and employs a multimodal skip-gram model to create vertex embeddings that aid in predicting user-item links. Metapath2vec is publicly accessible, with implementation details provided.

**DGRec (Session-guided Model):** DGRec merges a dynamic graph-attention neural network with a recurrent deep architecture to capture context-sensitive socially-aware influences and the evolution of user interests, respectively. This system combines these elements to provide tailored recommendations. DGRec's source code is also publicly available for download.

**LightFM:** Addressing the cold start problem, LightFM combines an MF model with item and client representations through linear combinations of hidden topics related

**TABLE 5. Max, Min, Avg photo counts and standard deviation per client for 45 new purchasing genres.**

Genre	Maximum	Minimum	Ave	Dev
Gaming Chairs	3450	15	245	40.5
Car Accessories	3680	25	258	42.0
Home Decor	3120	18	220	38.4
Pet Supplies	2950	12	201	34.8
Garden Tools	4200	28	298	49.6
Smart Lights	3750	22	268	45.2
Baby Monitors	2840	14	210	37.4
Musical Instruments	3670	26	265	43.0
Bicycles	3050	19	225	39.6
Fitness Equipment	4300	32	305	50.8
Backpacks	2980	13	215	35.6
Camping Gear	3220	18	235	40.0
Office Supplies	2920	16	208	36.5
Board Games	3110	14	218	37.8
Hair Accessories	2700	10	190	32.1
Luggage	3570	24	250	42.9
Headphones	3870	21	270	45.5
Smart Speakers	3750	23	268	43.8
Tablets	4210	27	310	51.2
Drones	3950	26	290	48.0
Kitchen Utensils	3070	17	230	38.9
Water Bottles	2820	12	200	34.2
Projectors	4100	30	299	49.5
Power Banks	3890	20	278	44.7
Gaming Consoles	4500	33	340	53.4
Smartphones	4680	29	345	54.2
Toys	2800	15	210	34.9
Electric Scooters	4800	34	365	56.0
Cameras	3850	22	270	44.0
Monitors	4320	28	320	50.8
Printers	3710	21	255	42.0
Baby Products	3180	17	240	40.1
Smart Thermostats	4620	25	335	53.0
Bluetooth Speakers	3910	20	280	45.1
Electric Bikes	4100	27	295	48.0
Grills	3420	18	245	41.0
Vacuum Cleaners	4580	32	325	52.0
Treadmills	4120	26	305	49.2
Kitchen Appliances	4820	34	375	58.0
Video Doorbells	3780	22	270	45.8
Streaming Devices	3900	23	280	46.0
Wireless Chargers	3640	19	260	43.5
Home Automation	4220	30	320	50.2
Air Fryers	3700	24	275	44.2

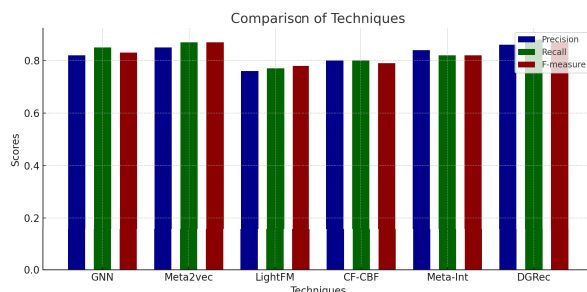
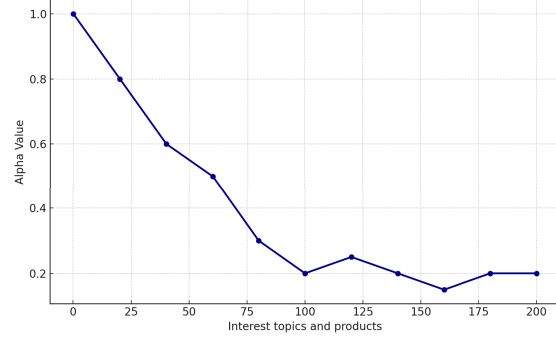
to purchasing-relevant attributes. It utilizes d-dimensional embeddings for each user and item feature, enhanced by scalar bias terms for each feature, to predict interactions via the dot product of their representations, adjusted for biases. LightFM's source code is available for public download.

**CF-CBF (Hybrid Filtering):** This method integrates user viewing habits and product similarities to determine a neighborhood set for recommending new items, blending content-based and collaborative filtering techniques.

For our assessments, we integrated the metadata-driven product recommendation approach into an existing socially-aware platform, Newsfulness5, previously developed for automated personality recognition projects. Newsfulness5 serves as a platform where users can access and share news content from various English-language publishers, and

**TABLE 6.** Balanced Error Rate (BER) values for the compared techniques.

Genre	K-means	Hierarchical	Link	Clique Per.	Low-rank	Multi-ass.	Our technique
Gaming Chairs	0.6520	0.4812	0.5216	0.6107	0.5628	0.5769	<b>0.4795</b>
Car Accessories	0.6105	0.4923	0.5302	0.6120	0.5431	0.5875	<b>0.4887</b>
Home Decor	0.6410	0.4579	0.5042	0.5714	0.5452	0.5786	<b>0.4803</b>
Pet Supplies	0.6637	0.4950	0.5218	0.5834	0.5648	0.5931	<b>0.4857</b>
Garden Tools	0.6842	0.5132	0.5554	0.5901	0.5748	0.6123	<b>0.5025</b>
Smart Lights	0.6340	0.4690	0.5164	0.5792	0.5567	0.5874	<b>0.4778</b>
Baby Monitors	0.6523	0.4887	0.5276	0.6002	0.5619	0.5832	<b>0.4782</b>
Musical Instruments	0.6789	0.5145	0.5479	0.6157	0.5812	0.6060	<b>0.4945</b>
Bicycles	0.6112	0.4698	0.5236	0.5894	0.5571	0.5726	<b>0.4793</b>
Fitness Equipment	0.6595	0.4956	0.5432	0.6080	0.5734	0.5917	<b>0.4912</b>
Backpacks	0.6190	0.4637	0.5109	0.5809	0.5525	0.5751	<b>0.4739</b>
Camping Gear	0.6417	0.4720	0.5225	0.5880	0.5599	0.5830	<b>0.4851</b>
Office Supplies	0.6225	0.4558	0.5091	0.5757	0.5461	0.5778	<b>0.4715</b>
Board Games	0.6389	0.4652	0.5180	0.5879	0.5563	0.5792	<b>0.4820</b>
Hair Accessories	0.6535	0.4875	0.5321	0.6048	0.5645	0.5896	<b>0.4903</b>
Luggage	0.6284	0.4726	0.5189	0.5921	0.5618	0.5850	<b>0.4822</b>
Headphones	0.6445	0.4793	0.5275	0.6022	0.5714	0.5953	<b>0.4864</b>
Smart Speakers	0.6320	0.4678	0.5224	0.5905	0.5561	0.5809	<b>0.4813</b>
Tablets	0.6512	0.4864	0.5342	0.6083	0.5690	0.5964	<b>0.4931</b>
Drones	0.6724	0.5012	0.5420	0.6115	0.5789	0.6073	<b>0.4980</b>
Kitchen Utensils	0.6187	0.4595	0.5159	0.5836	0.5527	0.5732	<b>0.4748</b>
Water Bottles	0.6095	0.4524	0.5071	0.5740	0.5443	0.5669	<b>0.4685</b>
Projectors	0.6751	0.5074	0.5443	0.6191	0.5821	0.6117	<b>0.5026</b>
Power Banks	0.6440	0.4823	0.5309	0.6057	0.5705	0.5924	<b>0.4889</b>
Gaming Consoles	0.6980	0.5212	0.5601	0.6254	0.5912	0.6207	<b>0.5106</b>
Smartphones	0.7123	0.5341	0.5756	0.6387	0.6010	0.6355	<b>0.5250</b>
Toys	0.6005	0.4459	0.4954	0.5669	0.5392	0.5585	<b>0.4623</b>
Electric Scooters	0.7202	0.5401	0.5812	0.6456	0.6117	0.6420	<b>0.5330</b>
Cameras	0.6564	0.4937	0.5345	0.6110	0.5735	0.6002	<b>0.4949</b>
Monitors	0.6693	0.5106	0.5470	0.6214	0.5856	0.6097	<b>0.5072</b>
Printers	0.6312	0.4805	0.5239	0.5995	0.5642	0.5880	<b>0.4847</b>
Baby Products	0.6247	0.4720	0.5192	0.5894	0.5570	0.5805	<b>0.4819</b>
Smart Thermostats	0.7103	0.5304	0.5705	0.6365	0.5984	0.6312	<b>0.5227</b>
Bluetooth Speakers	0.6415	0.4865	0.5293	0.6031	0.5689	0.5915	<b>0.4871</b>
Electric Bikes	0.6657	0.5032	0.5450	0.6152	0.5807	0.6065	<b>0.4984</b>
Grills	0.6301	0.4786	0.5217	0.5962	0.5634	0.5863	<b>0.4820</b>
Vacuum Cleaners	0.7180	0.5382	0.5796	0.6435	0.6098	0.6407	<b>0.5312</b>
Treadmills	0.6745	0.5060	0.5490	0.6197	0.5829	0.6112	<b>0.4995</b>
Kitchen Appliances	0.7340	0.5540	0.5953	0.6562	0.6223	0.6509	<b>0.5405</b>
Video Doorbells	0.6294	0.4791	0.5220	0.5964	0.5641	0.5870	<b>0.4818</b>
Streaming Devices	0.6407	0.4850	0.5285	0.6048	0.5711	0.5928	<b>0.4860</b>
Wireless Chargers	0.6286	0.4714	0.5187	0.5902	0.5580	0.5794	<b>0.4786</b>
Home Automation Systems	0.7193	0.5367	0.5785	0.6425	0.6080	0.6391	<b>0.5308</b>
Air Fryers	0.6541	0.4902	0.5365	0.6070	0.5710	0.5980	<b>0.4933</b>
<b>Ave.</b>	0.6585	0.4913	0.5348	0.6089	0.5732	0.5975	<b>0.4902</b>

**FIGURE 6.** Overall comparison of different recommendation systems.**FIGURE 7.** Recommendation performance by tuning parameter.

partake in a Big-Five character user study during onboarding. It aggregates content from major news outlets across multiple categories and tailors product suggestions by pulling data from online retailers like Jingdong (JD), Banggood, and

Amazon. Detailed dataset statistics are outlined in Table 7, with more comprehensive comparisons presented in Fig. 6 and 7.

**TABLE 7.** Statistics of our online product recommendation data set.

Parameter	Value
Client number	2235
Online Product number	25870
Number of items	6245
Cold start clients	585
Cold start clients	1520

## V. CONCLUSION AND SUMMARY OF FINDINGS

In this study, we devised a robust method to categorize extensive groups of clients into distinct communities, referred to as “genres,” rooted in their common purchasing behaviors. We developed an effective online product recommendation pipeline grounded in this classification. Our strategy employed a regularized topic modeling technique to precisely capture and depict each client’s purchasing patterns. This data was then used to create a comprehensive graph that delineates the aesthetic connections between users, thereby aiding in their organization into well-defined genres based on these relationships. Comparative evaluations have underscored the efficacy of our approach, demonstrating its potential in enhancing online product recommendation systems.

To further strengthen our approach, it is important to address potential limitations and future work areas, particularly in relation to parallelization and diverse datasets. As the scale of data grows in real-world applications, the computational complexity of graph-based clustering and regularized topic modeling may pose challenges. One potential area for improvement is the parallelization of key components in the pipeline, such as graph construction and model training, which could significantly enhance scalability and processing speed, especially when dealing with large datasets. Furthermore, while our method has proven effective on datasets with specific purchasing patterns, testing it on more diverse datasets—such as those with highly varied or sparse purchasing behaviors—could provide valuable insights into its adaptability and robustness. Future work may also focus on integrating dynamic data updates, allowing the system to continuously learn and adjust recommendations as user preferences evolve over time.

## REFERENCES

- [1] B. Zhou, A. Lapedriza, J. Xiao, A. Torralba, and A. Oliva, “Learning deep features for scene recognition using places database,” in *Proc. NIPS*, 2014, pp. 1–9.
- [2] J. Deng, W. Dong, R. Socher, L.-J. Li, K. Li, and L. Fei-Fei, “ImageNet: A large-scale hierarchical image database,” in *Proc. IEEE Conf. Comput. Vis. Pattern Recognit.*, Jun. 2009, pp. 248–255.
- [3] R. Achanta, A. Shajii, K. Smith, A. Lucchi, P. Fua, and S. Süsstrunk, “SLIC superpixels compared to state-of-the-art superpixel methods,” *IEEE Trans. Pattern Anal. Mach. Intell.*, vol. 34, no. 11, pp. 2274–2282, Nov. 2012.
- [4] L. Zhang, Y. Han, Y. Yang, M. Song, S. Yan, and Q. Tian, “Discovering discriminative graphlets for aerial image categories recognition,” *IEEE Trans. Image Process.*, vol. 22, no. 12, pp. 5071–5084, Dec. 2013.
- [5] F.-F. Li and P. Perona, “A Bayesian hierarchical model for learning natural scene categories,” in *Proc. IEEE Comput. Soc. Conf. Comput. Vis. Pattern Recognit.*, Jun. 2005, pp. 524–531.
- [6] J. Xiao, J. Hays, K. A. Ehinger, A. Oliva, and A. Torralba, “SUN database: Large-scale scene recognition from abbey to zoo,” in *Proc. IEEE Comput. Soc. Conf. Comput. Vis. Pattern Recognit.*, Jun. 2010, pp. 3485–3492.
- [7] S. Lazebnik, C. Schmid, and J. Ponce, “Beyond bags of features: Spatial pyramid matching for recognizing natural scene categories,” in *Proc. CVPR*, 2006, pp. 2169–2178.
- [8] A. Quattoni and A. Torralba, “Recognizing indoor scenes,” in *Proc. IEEE Conf. Comput. Vis. Pattern Recognit.*, Jun. 2009, pp. 413–420.
- [9] Y. Cong, J. Liu, J. Yuan, and J. Luo, “Self-supervised online metric learning with low rank constraint for scene categorization,” *IEEE Trans. Image Process.*, vol. 22, no. 8, pp. 3179–3191, Aug. 2013.
- [10] Y. Li, L. Liu, C. Shen, and A. van den Hengel, “Mid-level deep pattern mining,” in *Proc. CVPR*, 2015, pp. 971–980.
- [11] R. Girshick, J. Donahue, T. Darrell, and J. Malik, “Rich feature hierarchies for accurate object detection and semantic segmentation,” in *Proc. IEEE Conf. Comput. Vis. Pattern Recognit.*, Jun. 2014, pp. 580–587.
- [12] R. Wu, B. Wang, W. Wang, and Y. Yu, “Harvesting discriminative meta objects with deep CNN features for scene classification,” in *Proc. IEEE Int. Conf. Comput. Vis. (ICCV)*, Dec. 2015, pp. 1287–1295.
- [13] G. Piao and J. G. Breslin, “Inferring user interests in microblogging social networks: A survey,” *User Model. User-Adapted Interact.*, vol. 28, no. 3, pp. 277–329, Aug. 2018, doi: [10.1007/s11257-018-9207-8](https://doi.org/10.1007/s11257-018-9207-8).
- [14] F. Zarrinkalam, M. Kahani, and E. Bagheri, “Mining user interests over active topics on social networks,” *Inf. Process. Manage.*, vol. 54, no. 2, pp. 339–357, Mar. 2018.
- [15] A. K. Trikha, F. Zarrinkalam, and E. Bagheri, “Topic-association mining for user interest detection,” in *Proc. Eur. Conf. Inf. Retr.* Basel, Switzerland: Springer, 2018, pp. 665–671.
- [16] J. Wang, W. X. Zhao, Y. He, and X. Li, “Infer user interests via link structure regularization,” *ACM Trans. Intell. Syst. Technol.*, vol. 5, no. 2, pp. 1–22, Apr. 2014.
- [17] S. Dhelim, H. Ning, M. A. Bouras, and J. Ma, “Cyber-enabled human-centric smart home architecture,” in *Proc. IEEE SmartWorld, Ubiquitous Intell. Comput., Adv. Trusted Comput., Scalable Comput. Commun., Cloud Big Data Comput., Internet People Smart City Innov.*, Oct. 2018, pp. 1880–1886. [Online]. Available: <https://ieeexplore.ieee.org/document/8560294/>
- [18] S. Faralli, G. Stilo, and P. Velardi, “Automatic acquisition of a taxonomy of microblogs users’ interests,” *J. Web Semantics*, vol. 45, pp. 23–40, Aug. 2017.
- [19] S. Dhelim, N. Aung, and H. Ning, “Mining user interest based on personality-aware hybrid filtering in social networks,” *Knowl.-Based Syst.*, vol. 206, Oct. 2020, Art. no. 106227. [Online]. Available: <https://linkinghub.elsevier.com/retrieve/pii/S0950705120304354>
- [20] J. Kang and H. Lee, “Modeling user interest in social media using news media and Wikipedia,” *Inf. Syst.*, vol. 65, pp. 52–64, Apr. 2017.
- [21] Q. Liu, E. Chen, H. Xiong, C. H. Q. Ding, and J. Chen, “Enhancing collaborative filtering by user interest expansion via personalized ranking,” *IEEE Trans. Syst., Man, Cybern., B*, vol. 42, no. 1, pp. 218–233, Feb. 2012. [Online]. Available: <http://ieeexplore.ieee.org/document/6006538/>
- [22] C. Ye, J. Liu, C. Chen, M. Song, and J. Bu, “Speech emotion classification on a Riemannian manifold,” in *Proc. Pacific-Rim Conf. Multimedia*, 2008, pp. 61–69.
- [23] A. Krizhevsky, I. Sutskever, and G. E. Hinton, “ImageNet classification with deep convolutional neural networks,” in *Proc. NIPS*, 2012, pp. 1–9.
- [24] X. Zhu, Z. Ghahramani, and J. Lafferty, “Semi-supervised learning using Gaussian fields and harmonic functions,” in *Proc. ICML*, 2003, pp. 912–919.
- [25] C. Shi, Q. Ruan, G. An, and R. Zhao, “Hessian semi-supervised sparse feature selection based on  $L_{2,1/2}$ -matrix norm,” *IEEE Trans. Multimedia*, vol. 17, no. 1, pp. 16–28, Jan. 2015.
- [26] Y.-L. Boureau, J. Ponce, and Y. LeCun, “A theoretical analysis of feature pooling in visual recognition,” in *Proc. IEEE Int. Conf. Mach. Learn.*, Oct. 2010, pp. 111–118.
- [27] B. Cheng, B. Ni, S. Yan, and Q. Tian, “Learning to photograph,” in *Proc. 18th ACM Int. Conf. Multimedia*, Oct. 2010, pp. 291–300.
- [28] L. Zhang, M. Song, Q. Zhao, X. Liu, J. Bu, and C. Chen, “Probabilistic graphlet transfer for photo cropping,” *IEEE Trans. Image Process.*, vol. 22, no. 2, pp. 802–815, Feb. 2013.
- [29] L. Zhang, Y. Gao, C. Zhang, H. Zhang, Q. Tian, and R. Zimmermann, “Perception-guided multimodal feature fusion for photo aesthetics assessment,” in *Proc. 22nd ACM Int. Conf. Multimedia*, Nov. 2014, pp. 237–246.
- [30] D. M. Blei, A. Y. Ng, and M. I. Jordan, “Latent Dirichlet allocation,” *J. Mach. Learn. Res.*, vol. 3, pp. 993–1022, Mar. 2003.
- [31] W. H. Press, B. P. Flannery, S. A. Teukolsky, and W. T. Vetterling, *Numerical Recipes in C*. Cambridge, U.K.: Cambridge Univ. Press, 1998.

- [32] J. Quinlan, *C4.5 Programs for Machine Learning*. San Mateo, CA, USA: Morgan Kaufmann, 1993.
- [33] L. Zhang, C. Chen, J. Bu, D. Cai, X. He, and T. S. Huang, "Active learning based on locally linear reconstruction," *IEEE Trans. Pattern Anal. Mach. Intell.*, vol. 33, no. 10, pp. 2026–2038, Oct. 2011.
- [34] F. Pecune, L. Callebert, and S. Marsella, "A socially-aware conversational recommender system for personalized recipe recommendations," in *Proc. 8th Int. Conf. Human-Agent Interact.*, Nov. 2020, pp. 261–263.
- [35] J. Du, Z. Ye, L. Yao, B. Guo, and Z. Yu, "Socially-aware dual contrastive learning for cold-start recommendation," in *Proc. 45th Int. ACM SIGIR Conf. Res. Develop. Inf. Retr.*, Jul. 2022, pp. 1831–1835.
- [36] S. Konomi, K. Xu, Y. Chen, Y. Tang, and M. Bern, "Leveraging living trust networks for socially-aware recommendations," in *Proc. Conf. Human-Agent Interact.* Springer, 2023, pp. 22–32.
- [37] F. Pecune, L. Callebert, and S. Marsella, "Designing persuasive food conversational recommender systems with nudging and socially-aware conversational strategies," *Frontiers Robot. AI*, vol. 8, Jan. 2022, Art. no. 870211.
- [38] J. Yu, H. Yin, M. Gao, X. Xia, X. Zhang, and N. Q. Viet Hung, "Socially-aware self-supervised tri-training for recommendation," in *Proc. 27th ACM SIGKDD Conf. Knowl. Discovery Data Mining*, Aug. 2021, pp. 2559–2562.
- [39] M.-C. Lee and Y. P. Hong, "Socially-aware joint recommendation and caching policy design in wireless D2D networks," in *Proc. IEEE Int. Conf. Commun.*, Jun. 2021, pp. 1–6.
- [40] S. Dhelim, M. Aung, M. Bouras, and W. Hwang, "A survey on personality-aware recommendation systems," *Artif. Intell. Rev.*, vol. 55, pp. 2409–2454, Sep. 2022.
- [41] G. Costa and R. Ortale, "A Bayesian hierarchical approach for exploratory analysis of communities and roles in social networks," in *Proc. IEEE/ACM Int. Conf. Adv. Social Netw. Anal. Mining*, Aug. 2012, pp. 194–201.
- [42] E. Yao, G. Zheng, O. Jin, S. Bao, K. Chen, Z. Su, and Y. Yu, "Probabilistic text modeling with orthogonalized topics," in *Proc. 37th Int. ACM SIGIR Conf. Res. Develop. Inf. Retr.*, Jul. 2014, pp. 907–910.
- [43] D. Zhou, E. Manavoglu, J. Li, C. L. Giles, and H. Zha, "Probabilistic models for discovering e-communities," in *Proc. 15th Int. Conf. World Wide Web*, May 2006, pp. 173–182.
- [44] Z. Yin, L. Cao, Q. Gu, and J. Han, "Latent community topic analysis: Integration of community discovery with topic modeling," *ACM Trans. Intell. Syst. Technol.*, vol. 3, no. 4, p. 63, 2012.
- [45] S. C. Johnson, "Hierarchical clustering schemes," *Psychometrika*, vol. 32, no. 3, pp. 241–254, Sep. 1967.
- [46] N. Dalal and B. Triggs, "Histograms of oriented gradients for human detection," in *Proc. IEEE Comput. Soc. Conf. Comput. Vis. Pattern Recognit.*, Jun. 2005, pp. 886–893.
- [47] M. A. Stricker and M. Orengo, "Similarity of color images," *Proc. SPIE*, vol. 2420, pp. 381–392, Mar. 1995.
- [48] T. Hofmann, "Probabilistic latent semantic analysis," in *Proc. Uncert. Artif. Intell.*, 1999, pp. 289–296.
- [49] Y. Chen, "Combining SVMs with various feature selection strategies," in *Feature Extraction*. Berlin, Germany: Springer-Verlag, 2005.
- [50] G. Palla, I. Derényi, I. Farkas, and T. Vicsek, "Uncovering the overlapping community structure of complex networks in nature and society," *Nature*, vol. 435, no. 7043, pp. 814–818, Jun. 2005.
- [51] Y.-Y. Ahn, J. P. Bagrow, and S. Lehmann, "Link communities reveal multiscale complexity in networks," *Nature*, vol. 466, no. 7307, pp. 761–764, Aug. 2010.
- [52] T. Yoshida, "Toward finding hidden communities based on user profile," in *Proc. IEEE Int. Conf. Data Mining Workshops*, Dec. 2010, pp. 380–387.
- [53] M. Frank, A. P. Streich, D. Basin, and J. M. Buhmann, "Multi-assignment clustering for Boolean data," *J. Mach. Learn. Res.*, vol. 13, pp. 459–489, Feb. 2012.
- [54] H. Zhang, R. Edwards, and L. Parker, "Regularized probabilistic latent semantic analysis with continuous observations," in *Proc. 11th Int. Conf. Mach. Learn. Appl.*, Dec. 2012, pp. 560–563.
- [55] Z. Harchaoui and F. Bach, "Image classification with segmentation graph kernels," in *Proc. IEEE Conf. Comput. Vis. Pattern Recognit.*, Jun. 2007, pp. 1–8.
- [56] J. Wang, J. Yang, K. Yu, F. Lv, T. Huang, and Y. Gong, "Locality-constrained linear coding for image classification," in *Proc. IEEE Comput. Soc. Conf. Comput. Vis. Pattern Recognit.*, Jun. 2010, pp. 3360–3367.
- [57] J. Yang, K. Yu, Y. Gong, and T. Huang, "Linear spatial pyramid matching using sparse coding for image classification," in *Proc. IEEE Conf. Comput. Vis. Pattern Recognit.*, Jun. 2009, pp. 1794–1801.
- [58] L.-J. Li, H. Su, E. P. Xing, and L. Fei-Fei, "Object bank: A high-level image representation for scene classification and semantic feature sparsification," in *Proc. NIPS*, 2010, pp. 1–9.
- [59] X. Zhou, K. Yu, T. Zhang, and T. S. Huang, "Image classification using super-vector coding of local image descriptors," in *Proc. ECCV*, 2010, pp. 141–154.
- [60] J. Yang, K. Yu, and T. S. Huang, "Supervised translation-invariant sparse coding," in *Proc. CVPR*, 2010, pp. 3517–3524.
- [61] D. Song and D. Tao, "Biologically inspired feature manifold for scene classification," *IEEE Trans. Image Process.*, vol. 19, no. 1, pp. 174–184, Jan. 2010.
- [62] E. Hadjidemetriou, M. D. Grossberg, and S. K. Nayar, "Multiresolution histograms and their use for recognition," *IEEE Trans. Pattern Anal. Mach. Intell.*, vol. 26, no. 7, pp. 831–847, Jul. 2004.
- [63] K. He, X. Zhang, S. Ren, and J. Sun, "Spatial pyramid pooling in deep convolutional networks for visual recognition," *IEEE Trans. Pattern Anal. Mach. Intell.*, vol. 37, no. 9, pp. 1904–1916, Sep. 2015.
- [64] H.-C. Yang and Z.-R. Huang, "Mining personality traits from social messages for game recommender systems," *Knowl.-Based Syst.*, vol. 165, pp. 157–168, Feb. 2019. [Online]. Available: <https://linkinghub.elsevier.com/retrieve/pii/S095070511830577X>
- [65] P. Xu, F. Roosta, and M. W. Mahoney, "Newton-type methods for non-convex optimization under inexact Hessian information," *Math. Program.*, vol. 184, nos. 1–2, pp. 35–70, Nov. 2020.
- [66] W. Wu, L. Chen, and Y. Zhao, "Personalizing recommendation diversity based on user personality," *User Model. User-Adapted Interact.*, vol. 28, no. 3, pp. 237–276, Aug. 2018.
- [67] H. Ning, S. Dhelim, and N. Aung, "PersoNet: Friend recommendation system based on big-five personality traits and hybrid filtering," *IEEE Trans. Computat. Social Syst.*, vol. 6, no. 3, pp. 394–402, Jun. 2019. [Online]. Available: <https://ieeexplore.ieee.org/document/8675299/>
- [68] B. Ferwerda, M. Tkalcic, and M. Schedl, "Personality traits and music genres: What do people prefer to listen to?" in *Proc. 25th Conf. User Model. Adaptation Personalization*, Jul. 2017, pp. 285–288.
- [69] B. Ferwerda, E. Yang, M. Schedl, and M. Tkalcic, "Personality and taxonomy preferences, and the influence of category choice on the user experience for music streaming services," *Multimedia Tools Appl.*, vol. 78, no. 14, pp. 20157–20190, Jul. 2019.
- [70] Z. Yusefi Hafshejani, M. Kaedi, and A. Fatemi, "Improving sparsity and new user problems in collaborative filtering by clustering the personality factors," *Electron. Commerce Res.*, vol. 18, no. 4, pp. 813–836, Dec. 2018.
- [71] S. Dhelim, N. Huansheng, S. Cui, M. Jianhua, R. Huang, and K. I.-K. Wang, "Cyberentity and its consistency in the cyber-physical-social-thinking hyperspace," *Comput. Electr. Eng.*, vol. 81, Jan. 2020, Art. no. 106506.
- [72] A. Khelloufi, H. Ning, S. Dhelim, T. Qiu, J. Ma, R. Huang, and L. Atzori, "A social-relationships-based service recommendation system for SIoT devices," *IEEE Internet Things J.*, early access, Aug. 14, 2020, doi: [10.1109/JIOT.2020.3016659](https://doi.org/10.1109/JIOT.2020.3016659).
- [73] P. Arbeláez, J. Pont-Tuset, J. Barron, F. Marques, and J. Malik, "Multiscale combinatorial grouping," in *Proc. IEEE Conf. Comput. Vis. Pattern Recognit.*, Jun. 2014, pp. 328–335.
- [74] G. Mesnil, S. Rifai, A. Bordes, X. Glorot, Y. Bengio, and P. Vincent, "Unsupervised learning of semantics of object detections for scene categorizations," in *Proc. PRAM*, 2015, pp. 163–177.
- [75] Y. Xiao, J. Wu, and J. Yuan, "mCENTRIST: A multi-channel feature generation mechanism for scene categorization," *IEEE Trans. Image Process.*, vol. 23, no. 2, pp. 823–836, Feb. 2014.

**NAN SU** was born in Zhengzhou, Henan, China, in 1990. She received the bachelor's degree from the Curtin University of Australia, in January 2011, and the master's degree from Monash University of Australia, in May 2012. From 2013 to 2014, she was an Associate Analyst with Beijing MyFP Corporation. Currently, she is with Zhengzhou Shengda University. She has published several articles and participated in many projects. Her research interests include equity market, commercial banking, green finance, and the use of AI for finance and trade.